Draft version May 19, 2016
Preprint typeset using LaTeX style emulateapj v. 12/16/11

THE INFLUENCE OF SPIRAL ARMS ON ACTION-BASED DYNAMICAL MILKY WAY DISK MODELLING

Wilma H. Trick[1,2], Jo Bovy[3], Elena D'Onghia???, and Hans-Walter Rix[1]

Draft version May 19, 2016

ABSTRACT

- One sentence on what RoadMapping is.
- Overall axisymmetric RoadMapping modelling works in the presence of non-axisymmetric spiral arms, as long as the volume is big enough.

Keywords: Galaxy: disk — Galaxy: fundamental parameters — Galaxy: kinematics and dynamics — Galaxy: structure — [TO DO]

1. INTRODUCTION

- Explain what RoadMapping is, also Acronym
- Summarize BR13
- Summarize results of Paper 1, mention that non-axisymmetries were not considered there
- Main question: Does axisymmetric RoadMapping modelling work in the presence of non-axiysmmetric spiral arms?
- Consequences: Both potential and orbit DF are not axisymmetric, i.e., the fitted axisymmetric potential model and DF do per se not contain the truth.
- How to approach this: Use simulation by D'Onghia et al. 2013 and apply RM to it
- The potential model we use is chosen mostly for practical reasons and is not necessarily the optimal one for the simulation. Also, we use a single qDF as DF - because it is the simplest thing to do. Also independently of the non-axisymmetries the chosen models might deviate from the truth. Where we investigated deviations between model and truth in isolated test cases, here several assumptions break down simultaneously.
- Explain actions very shortly. $\boldsymbol{J} = (J_R, J_\phi = L_z, J_z)$ quantify oscillation in the coordinate directions (R, ϕ, z). Are calculated from current phase-space position in a given potential Φ.
- Say that actions are conserved in an axisymmetric potential, but not in non-axisymmetric potentials. (Maybe the mean vertical action is conserved [TO DO: Reference].) It is therefore important to check, if our modelling works in a system where actions are not conserved.

[1] Max-Planck-Institut für Astronomie, Königstuhl 17, D-69117 Heidelberg, Germany
[2] Correspondence should be addressed to trick@mpia.de.
[3] Department of Astronomy and Astrophysics, University of Toronto, 50 St. George Street, Toronto, ON, M5S 3H4, Canada

2. ROADMAPPING MODELLING

2.1. *Likelihood*

The data that goes into the modelling are the 6D position and velocity coordinates $(\boldsymbol{x}_i, \boldsymbol{v}_i)$ of N_* stars within the survey volume. For simplicity we use a purely spatial selection function $\mathrm{sf}(\boldsymbol{x})$ of spherical shape,

$$\mathrm{sf}(\boldsymbol{x}) \equiv \begin{cases} 1 & \text{if } |\boldsymbol{x} - \boldsymbol{x}_0| \leq r_{\max} \\ 0 & \text{otherwise} \end{cases},$$

whose maximum radius $r_{\max}$ defines the boundary of the survey volume and which is centred on $\boldsymbol{x}_0 \equiv (R_0, \phi_0, z_0 = 0)$. Given a parametrized potential model $\Phi(R, z)$ with parameters p_Φ, the i-th star is on an orbit characterized by the orbital actions

$$\boldsymbol{J}_i \equiv \boldsymbol{J}[\boldsymbol{x}_i, \boldsymbol{v}_i \mid p_\Phi].$$

The probability of stars to be on the orbit $\boldsymbol{J}_i$ is proportional to a given orbit distribution function $\mathrm{df}(\boldsymbol{J})$ with parameters p_{DF},

$$\mathrm{df}(\boldsymbol{J}_i \mid p_{\mathrm{DF}}) \equiv \mathrm{df}(\boldsymbol{J}[\boldsymbol{x}_i, \boldsymbol{v}_i \mid p_\Phi] \mid p_{\mathrm{DF}}) \equiv \mathrm{df}(\boldsymbol{x}_i, \boldsymbol{v}_i \mid p_\Phi, p_{\mathrm{DF}}),$$

where the latter equivalence arises from the Jacobian determinant between the angle-action coordinates $(\boldsymbol{\theta}, \boldsymbol{J})$ and cartesian phase-space coordinates $(\boldsymbol{x}, \boldsymbol{v})$, which is $|\partial(\boldsymbol{x}, \boldsymbol{v})/\partial(\boldsymbol{\theta}, \boldsymbol{J})| = 1$ and therefore allows us to treat the df equivalently as a distribution of current phase-space coordinates or a distribution of orbital actions only, with uniform distribution in the angles $\boldsymbol{\theta}$. In some sense, the $\mathrm{df}(\boldsymbol{J})$ describes how we expect a realistic stellar population in the MW disk to look like.

The joint likelihood of the i-th star being on an orbit $\boldsymbol{J}$ in the potential Φ and being within the survey volume is therefore

$$\mathscr{L}_i \equiv \mathscr{L}(\boldsymbol{x}_i, \boldsymbol{v}_i) = \frac{\mathrm{df}(\boldsymbol{x}_i, \boldsymbol{v}_i \mid p_\phi, p_{\mathrm{DF}}) \cdot \mathrm{sf}(\boldsymbol{x_i})}{\int \mathrm{df}(\boldsymbol{x}, \boldsymbol{v} \mid p_\Phi, p_{\mathrm{DF}}) \cdot \mathrm{sf}(\boldsymbol{x}) \ \mathrm{d}^3x\, \mathrm{d}^3v}.$$

The details how we evaluate the likelihood normalisation numerically to sufficiently high enough precision are discussed in Paper I.[4]

In the scenario considered in this paper it can happen that there are a few ($\sim$ 1 in 20,000) stars entering the

[4] [TO DO: Write what exact numerical accuracy we use and check that it is actually good enough.]

catalogue that are for some reason on rather extreme orbits, e.g., moving radially directly towards the center. These kinds of orbits do not belong to the set of orbits that we classically expect to make up a overall smooth galactic disk. To avoid that such single stars with very low likelihood mess up the modelling we introduce here a simple outlier model,

$$\mathscr{L}_i \longrightarrow \max\left(\mathscr{L}_i, \epsilon \cdot \mathrm{median}(\mathscr{L})\right),$$

where $\epsilon = 0.001$ for $N_* = 20,000$ stars and median($\mathscr{L}$) is the median of all the N_* stellar likelihoods $\mathscr{L}_i$ with the given p_Φ and $p_{\rm DF}$. This outlier model was not used in Paper I.

Following Paper I, we assume for now uninformative flat priors on the model parameters p_Φ and $p_{\rm DF}$ and find the maximum and width of the posterior probability function

$$pdf(p_\Phi, p_{\rm DF} \mid \mathrm{data}) \propto \prod_{i=1}^{N_*} \mathscr{L}_i \cdot prior(p_\Phi, p_{\rm DF})$$

using a nested-grid approach and then explore the full shape of the *pdf* using a Monte Carlo Markov Chain (MCMC)[5]. Full details on this procedure are given in Paper I.

2.2. *DF model*

The most simple orbit distribution function exhibiting a disk-like structure may be the quasi-isothermal distribution function (qDF) introduced by Binney (2010) and Binney & McMillan (2011). It proofed to be a successful model to describe the orbit distribution of individual mono-abundance populations (MAPs) in the Galactic disk (Bovy & Rix 2013; Ting et al. 2013), that seem to be isothermal in z-direction (i.e., "quasi-isothermal"). Modelling approaches trying to capture the overall disk distribution (Piffl et al. 2014; Sanders & Binney 2015) were describing the Galactic disk as a superposition of many qDFs. The qDF, which we already used in Paper I, has the functional form

$$\begin{aligned}&\mathrm{qDF}(\boldsymbol{J} \mid p_{\rm DF})\\ &= f_{\sigma_R}\left(J_R, L_z \mid p_{\rm DF}\right) \times f_{\sigma_z}\left(J_z, L_z \mid p_{\rm DF}\right)\end{aligned} \tag{1}$$

where

$$\begin{aligned}f_{\sigma_R}\left(J_R, L_z \mid p_{\rm DF}\right) = n \times \frac{\Omega}{\pi\sigma_R^2(R_g)\kappa} \exp\left(-\frac{\kappa J_R}{\sigma_R^2(R_g)}\right)\\ \times\left[1 + \tanh\left(L_z/L_0\right)\right]\end{aligned} \tag{2}$$

$$f_{\sigma_z}\left(J_z, L_z \mid p_{\rm DF}\right) = \frac{\nu}{2\pi\sigma_z^2(R_g)} \exp\left(-\frac{\nu J_z}{\sigma_z^2(R_g)}\right) \tag{3}$$

(Binney & McMillan 2011). The guiding-center radius R_g, circular frequency Ω, radial/epicycle frequency κ and vertical frequency ν describe the near-circular orbit with given angular momentum L_z in a given potential. Counter-rotating orbits with $L_z < L_0$ are suppressed by the term $\left[1 + \tanh\left(L_z/L_0\right)\right]$ (with $L_0 \sim 10$ km s^{-1} kpc). We set the radial stellar tracer density $n(R_g)$ and velocity dispersion profiles $\sigma_z(R_g)$ and $\sigma_R(R_g)$ to

$$n(R_g \mid p_{\rm DF}) \propto \exp\left(-\frac{R_g}{h_R}\right) \tag{4}$$

$$\sigma_R(R_g \mid p_{\rm DF}) = \sigma_{R,0} \times \exp\left(-\frac{R_g - R_\odot}{h_{\sigma,R}}\right) \tag{5}$$

$$\sigma_z(R_g \mid p_{\rm DF}) = \sigma_{z,0} \times \exp\left(-\frac{R_g - R_\odot}{h_{\sigma,z}}\right). \tag{6}$$

The free model parameters of the qDF are therefore

$$p_{\rm DF} \equiv \left\{\ln h_R, \ln\sigma_{R,0}, \ln\sigma_{z,0}, h_{\sigma,R}, h_{\sigma,z}\right\}.$$

Even though we do not have any stellar abundance or age information in the simulation snapshot we are going to investigate (see Section 3) and we therefore cannot define stellar sub-populations for which the assumption of such a simple model might be reasonable, we will still try to model the whole disk with a single qDF—to see how far we can get with the simplest possible model.

2.3. *Potential model*

- Introduce potential model, explain that form of disk was mostly chosen to the closed form expression of *Phi* which allows for fast calculation. Both MNHH, DEHH and KKS pot.
- Mention action calculation and that we tested explicitely that fixing Delta=0.45 and using staeckel interpolation grid does not degrade the analysis
- Mention and reference galpy.

3. DATA FROM A GALAXY SIMULATION

3.1. *Description of the galaxy simulation*

We use a high-resolution N-body simulation of a disk galaxy by D'Onghia et al. (2013) carried out with GADGET-3 code described in Springel et al. (2005), in which overdensities with properties similar to giant molecular clouds induced prominent spiral arms—and therefore non-axisymmetric sub-structure—via the swing amplification mechanism.

For details see D'Onghia et al. (2013), here we summarize the essential characteristics.

The simulation has a gravitationally evolving stellar disk within a static/rigid analytic dark matter halo.

The analytic halo follows a Hernquist (1990) profile

$$\rho_{\rm dm}(r) = \frac{M_{\rm dm}}{2\pi} \frac{a_{\rm dm}}{r(r + a_{\rm dm})^3} \tag{7}$$

with total halo mass $M_{\rm dm} = 9.5 \cdot 10^{11}\ M_\odot$ and scale length $a_{\rm dm} = 29$ kpc (Elena D'Onghia, private communication). [There is no way to check that this is indeed the case. What should I do?]

The disk consists of 10^8 "disk star" particles, each having a mass of 370 $M_\odot$, and 1000 "giant molecular cloud" particles with mass $9.5 \cdot 10^5\ M_\odot$. Initially the particles are distributed following an exponential disk profile with density

$$\rho_*(R, z) = \frac{M_*}{4\pi z_0 R_s^2} \mathrm{sech}^2\left(\frac{z}{z_0}\right) \exp\left(-\frac{R}{R_s}\right),$$

[5] [TO DO: Reference emcee]

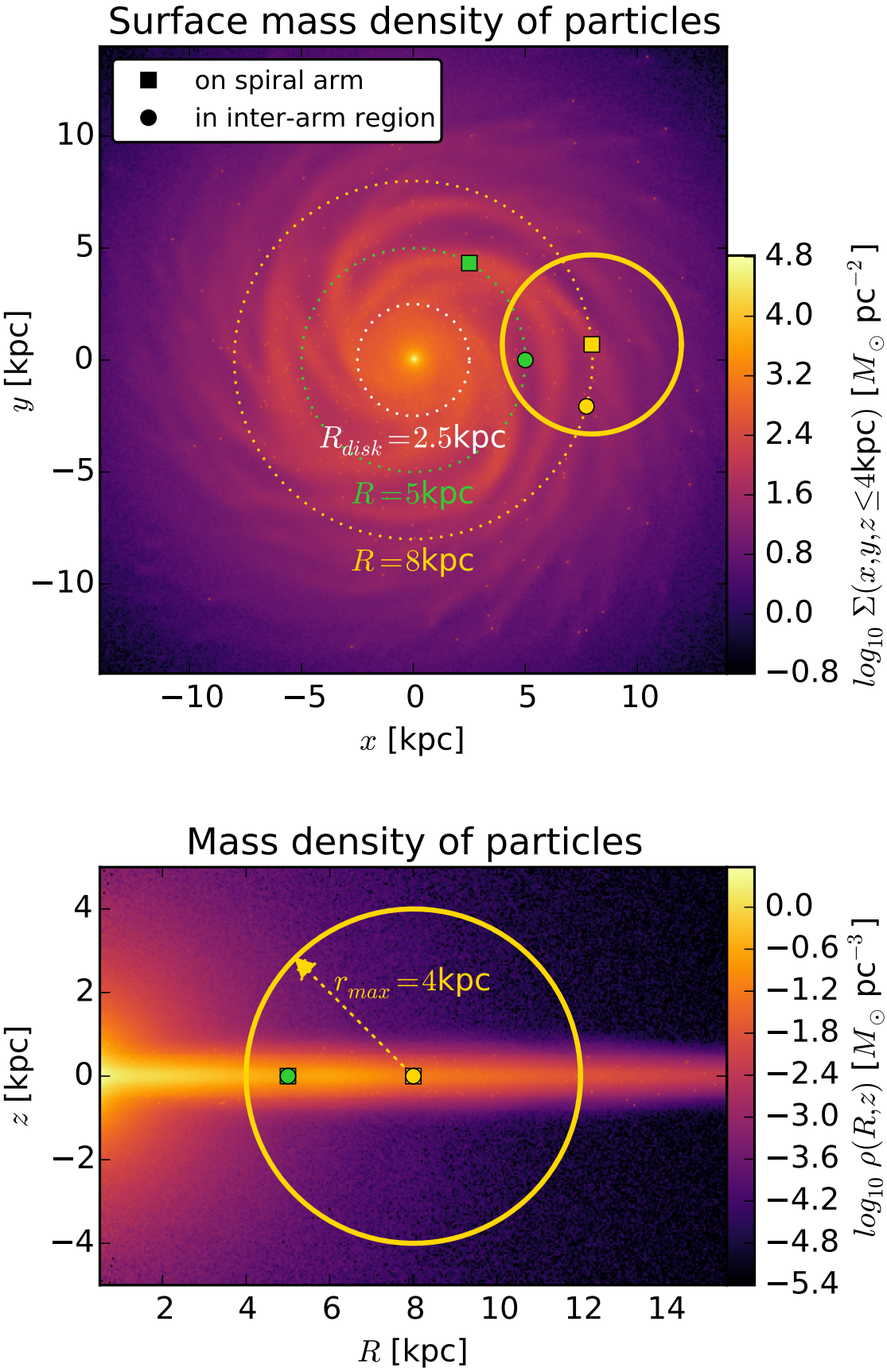
Surface mass density of particles
on spiral arm
in inter-arm region
R_{disk}=2.5kpc
R=5kpc
R=8kpc
y [kpc]
x [kpc]
$log_{10}\,\Sigma(x,y,z\leq$4kpc$)$ [$M_\odot$ pc^{-2}]
Mass density of particles
r_{max}=4kpc
z [kpc]
R [kpc]
$log_{10}\,\rho(R,z)$ [$M_\odot$ pc^{-3}]

Figure 1.

with $R_s = 2.5$ kpc and $z_0 = 0.1 R_s$ [TO DO: Check in my own measurements] and total disk mass $M_* = 0.04 \cdot M_{\rm dm}$ [TO DO??? In Email from August 2011].

The bulge consists of 10^7 "bulge star" particles with mass 950 $M_\odot$ and they are distributed following a spherical Hernquist profile analogous to Equation (7), with total mass $M_{\rm bulge} = 0.01 \cdot M_{\rm dm} =$??? and scale length $a_{\rm bulge} = 0.1 \cdot R_s = 0.25$ kpc.

The simulation snapshot which we are using in this work has evolved under its own gravity for ~ 250 Myr. The mass density of simulation particles (without the DM halo) at this snapshot time is shown in Figure 1. Pronounced spiral arms have developed due to the "molecular cloud perturbers", which can be seen in Figure 1 as small overdensities in the disk. The spherical bulge and very flattened disk are shown in the lower panel in Figure 1.

We have confirmed that the gravitational center of the particles corresponds to the coordinate origin.

3.2. *Survey volume and data*

- Mention that we do not consider any measurement errors

3.3. *Symmetrized potential model*

3.4. *Quantifying influence of spiral arm*

[TO DO: There is a short comment on that in D'Onghia 2013 as well]

4. RESULTS

4.1. *A single application of RoadMapping*

4.1.1. *Fiducial test*

- $r_{max} = 4kpc$
- $N_* = 20,000$
- MNHH potential

4.1.2. *Recovering the stellar distribution*

- Figure: (x,y) and (R,z) distribution of residuals of true and best fit stellar distribution. Mark spiral arms as circles with radius Rg.
- Figure: 1D histograms in R,z,phi, comparison of true, best fit and best fit in symmetrized potential
- Figure: 1D histograms in velocity and different (R,z,phi) bins comparison of true, best fit and best fit in symmetrized potential

4.1.3. *Recovering the potential*

- Figure: density overview plot
- Figure: vcirc, surfdens overview plot
- Figure: local potential overview plot, scatter plot of stars color coded according to deviation of true and best fit (maybe also symmetrized) potential. normalize potential such that at solar circle pot=0. Both in % of true potential and number of sigma away.
- Figure: forces overview plot, incl. local forces scatter plot
- Discuss somehow that the model parameters are actually themselves not very good recovered. Maybe violin plot?

4.1.4. *Recovering the action distribution*

- Figure: residuals in action space, comparison of true/symmetrized vs. best fit actions (maybe also true vs. best fit in symmetrized potential), overplot Lz=vcirc*Rg of spiral arms

4.2. *Investigation of different aspects*

4.2.1. *Test suite*

- $r_{max} = 1, 2, 3, 4, 5kpc$
- $N_* = 20,000$
- MNHH potential + KKS potential
- $R_{obs} = 5and8kpc$

4.2.2. *Survey volume and choice of potential model*

- Figure: x-axis: r_{max}, y-axis: one panel with mean stellar rms deviation in FR and one with Fz. With different potentials and r_{max}.

4.2.3. *Influence of spiral arms*

- Figure: x-axis: $\langle\kappa\rangle$, y-axis: one panel with mean stellar rms deviation in FR and one with Fz. Analyses with same potential but at different positions and sizes within the galaxy.
- Figure: x-axis: $sigma_\kappa$, y-axis: same as above figure.

5. SUMMARY AND CONCLUSION

REFERENCES

Binney, J. 2010, MNRAS, 401, 2318
Binney, J., & McMillan, P. 2011, MNRAS, 413, 1889
Bovy, J., & Rix, H.-W. 2013, ApJ, 779, 115
D'Onghia, E., Vogelsberger, M., & Hernquist, L. 2013, ApJ, 766, 34
Hernquist, L. 1990, ApJ, 356, 359
Piffl, T., Binney, J., McMillan, P. J., et al. 2014, MNRAS, 445, 3133
Sanders, J. L., & Binney, J. 2015, MNRAS, 449, 3479
Springel, V., Di Matteo, T., & Hernquist, L. 2005, MNRAS, 361, 776
Ting, Y.-S., Rix, H.-W., Bovy, J., & van de Ven, G. 2013, MNRAS, 434, 652

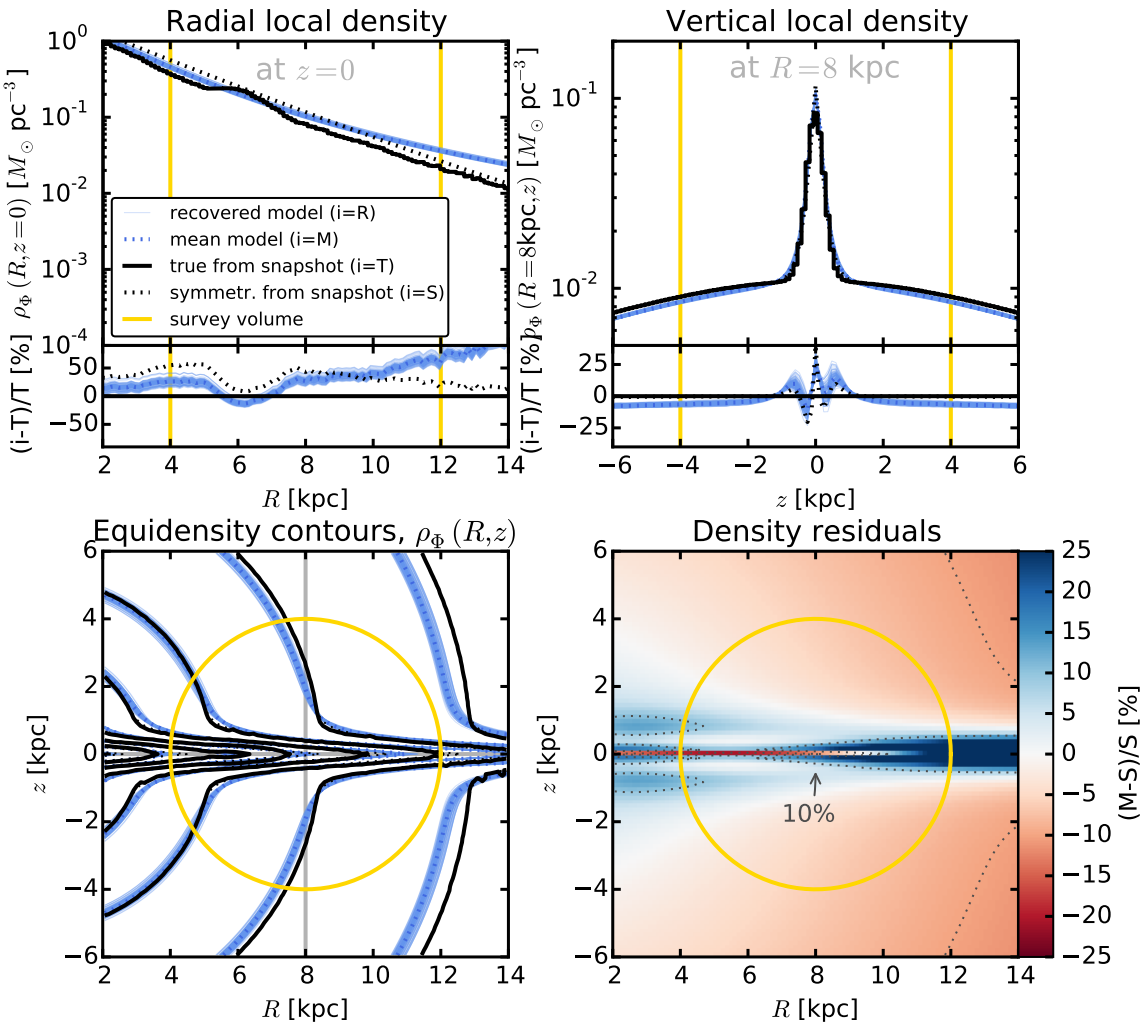

Figure 2. Comparison of the true density distribution $\rho_{\Phi,\mathrm{T}}$ in the galaxy simulation snapshot (solid black line, averaged over ϕ) with the axisymmetric density distribution $\rho_{\Phi,\mathrm{R}}$ recovered with *RoadMapping* (solid blue lines) from $N_* = 20,000$ stars in the survey volume with $r_{\max} = 4$ kpc (yellow line), as described in Section [TO DO]. The first two panels show density profiles along $(R, z = 0)$ and $(R = 8\ \mathrm{kpc}, z)$, together with the relative differences between true and recovered ρ_Φ. The third panel displays equidensity contours of the matter distribution in the (R, z) plane. Overplotted are also the symmetrized "true potential's $\rho_{\Phi,\mathrm{S}}$ (dotted black line) (see Section [TO DO]) and the $\rho_{\Phi,\mathrm{M}}$ of the recovered mean model in Table [TO DO] (dotted blue line). The last panel shows the relative difference between the symmetrized "true $\rho_{\Phi,\mathrm{S}}$ and the recovered mean model $\rho_{\Phi,\mathrm{M}}$. Over wide areas even outside of the survey volume the relative difference is less than 10%. At $R \gtrsim 8$ kpc and $z \sim 0$ it becomes apparent that the chosen potential model cannot perfectly capture the structure of the disk. [TO DO: Make sure that this plot actually contains the final analysis and sym. model that I want to show.] [TO DO: Maybe it would be more interesting to see a best fit MNd directly to the potential to see, how well the potential model can actually perform?] [TO DO: Maybe use only stars in the cone that the survey volume probes???]

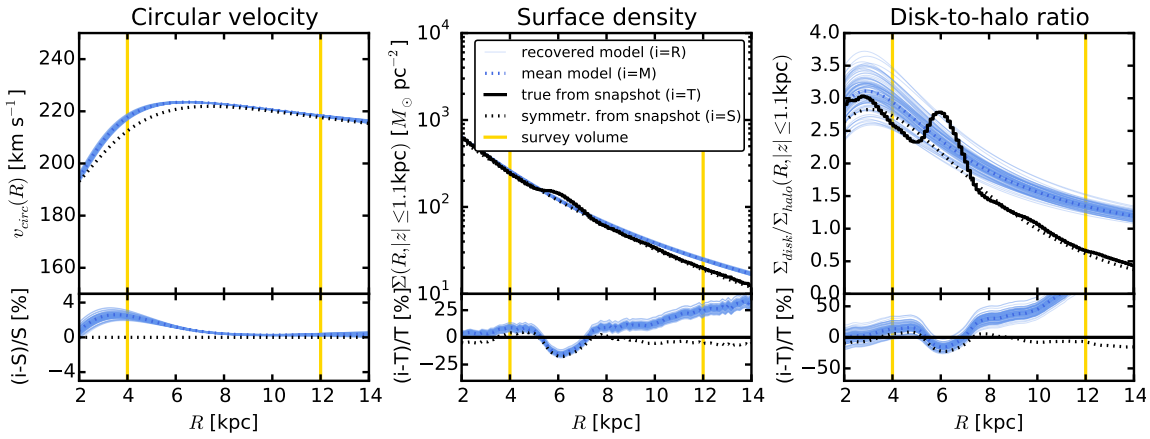

Figure 3. Comparison of the circular velocity curve, surface density profile within $|z| \leq 1.1$ kpc and disk-to-halo ratio of the surface density along R for the true potential of the galaxy simulation snapshot (solid black line) and the axisymmetric model potential recovered with *RoadMapping* (solid blue lines) (see Section [TO DO]). Overplotted are also the profiles of the symmetrized "true potential (dotted black line) (see Section [TO DO]) and the recovered mean model (dotted blue line) (see Table [TO DO]). The circular velocity curve is recovered to less than 5%, especially at larger radii. For the surface density and disk-to-halo ratio *RoadMapping* recovers the truth at radii $\lesssim 8$ kpc. The deviations at larger radii are connected to the discrepancies in the density in Figure [TO DO]. [TO DO: When I have the force I can probably also calculate the true circular velocity curve!]